Proceedings of the ASME 2010 3rd Joint US-European Fluids Engineering Summer Meeting and 8th International Conference on Nanochannels, Microchannels, and Minichannels
FEDSM-ICNMM2010
August 1-5, 2010, Montreal, Canada

FEDSM-ICNMM2010-30787

A VORTEX IMMERSED BOUNDARY METHOD FOR BLUFF BODY FLOWS

Georges-Henri Cottet
LJK - Tour IRMA
51, rue des Mathématiques
F-38041 Grenoble Cedex 9 FRANCE
Georges-Henri.Cottet@imag.fr

Federico Gallizio
DIASP - Politecnico di Torino
C.so Duca degli Abruzzi, 24
10129 Torino ITALY
federico.gallizio@polito.it

Optimad engineering srl
via Giacinto Collegno, 18
10143 Torino ITALY

Adrien Magni
LJK - Tour IRMA
51, rue des Mathématiques
F-38041 Grenoble Cedex 9 FRANCE
Adrien.Magni@imag.fr

Iraj Mortazavi
IMB Université de Bordeaux
MC^2 INRIA Bordeaux Sud-Ouest
351, cours de la Libération
F-33405 Talence FRANCE
mortaz@math.u-bordeaux1.fr

ABSTRACT

The aim of this work is to couple vortex methods with the penalization methods in order to take advantage from both of them. This immersed boundary approach maintains the efficiency of vortex methods for high Reynolds numbers focusing the computational task on the rotational zones and avoids their lack on the no-slip boundary conditions replacing the vortex sheet method by the penalization of obstacles. This method that is very appropriate for bluff-body flows is validated for the flow around a circular cylinder on a wide range of Reynolds numbers.

NOMENCLATURE

$\mathbf{u} = (u, v)$, p velocity field and pressure
Re Reynolds number
St Strouhal number
D computational domain
F, S fluid domain and solid domain
$\bar{\mathbf{u}}$ body rigid motion
u_∞ free stream velocity
C_L lift coefficient
C_D drag coefficient
d non-dimensional diameter
h reference mesh size
f vortex shedding frequency
λ penalization parameter
ω vorticity field
ν kinematic viscosity
ψ stream function
χ characteristic function
Δt time step

INTRODUCTION

Vortex methods (see [Cottet and Koumoutsakos 00] and [Mortazavi and Giovannini 01]) and penalization methods (see

[Angot et al. 1999] and [Bruneau et al. 2008]) have been separately used to compute incompressible high Reynolds number flows around obstacles. In this work, a novel hybrid particle-penalization technique is proposed to achieve efficient computations of bluff-body flows designing a more efficient technique that covers the advantages of both approaches. In this approach, the vortex method is used to approximate the penalized Vorticity Transport Equations (VTE). This technique that permits to solve the flow equations in a fast lagrangian way, overcomes the difficulty of the vortex methods to satisfy accurately the no-slip boundary conditions, introducing the penalization term in the Vorticity Transport Equations. Here, the idea is to extend the fluid velocity inside the solid body and to solve the flow equations with a penalization term to enforce rigid motion inside the solid, using a vorticity formulation. The main interest of the penalized vorticity formulation is that it replaces the usual vorticity creation algorithm in order to satisfy the no-slip boundary condition for vortex methods. This new technique avoids the convergence difficulties due to the creation of the particles on the solid boundaries. This approach is also able to take into account the moving obstacles and boundaries in the flow thanks to an immersed boundary algorithm that is used to complement this hybrid technique as shown in [Coquerelle et al 06] and [Coquerelle and Cottet 08]. Then, the method is validated for two-dimensional flows around a circular cylinder for a wide range of Reynolds numbers.

1 PENALIZATION METHOD FOR VELOCITY FORMULATION

Before all, we show how the penalization method can be used successfully to model the flow of an incompressible fluid around an obstacle [Angot et al. 1999]. In the penalization technique the system is considered as a single flow, subject to the Navier-Stokes equation with a penalization term that enforces continuity at the solid-fluid interface and rigid motion inside the solid. We solve simultaneously the Brinkman equations in the solid and the Navier-Stokes equations in the fluid, considering whole the domain as a porous medium with zero (solid) or infinite permeabilities (fluid). The main advantage of this method is that it needs neither the mesh to fit the boundaries nor to specify no-slip boundary conditions. In addition it allows to compute the pressure as a continuous field on the whole domain including the solids, and the lift and drag coefficients by integrating the penalization term inside the solid bodies [Bruneau et al. 2008].
The zone variation is realized changing the penalization coefficient that defines the permeability of each region. Numerically, the fluid is considered as a porous medium with a very high permeability ($K = 10^{16}$) and the bodies are considered as porous media with a very small permeability ($K = 10^{-8}$) . Let us define a penalization parameter $\lambda \approx 1/K$, that is $\lambda \to 0$ in the fluid region F and $\lambda >> 1$ in the solid region S. The full domain including the solid body is defined as $D = F \cup S$. By means of the λ, the velocity term is penalized for a solid in Brinkman equations. That means that Navier-Stokes equations are replaced by the following equations:

$$\partial_t \mathbf{u} + (\mathbf{u}\cdot\nabla)\mathbf{u} - \nu\Delta\mathbf{u} + \lambda\mathbf{u} + \nabla p = 0 \;\; in\; D \tag{1}$$

$$div\,\mathbf{u} = 0 \;\; in\; D \tag{2}$$

where λ is the penalization parameter with the dimension $[s^{-1}]$.

2 PENALIZATION METHOD FOR VORTICITY FORMULATION

In this section, the idea is to extend the fluid velocity inside the solid body and to solve the flow equations with a penalization term to enforce rigid motion inside the solid, using a vorticity formulation. The main interest of the penalized vorticity formulation is that it replaces the usual vorticity creation algorithm in order to satisfy the no-slip boundary condition for vortex methods. This new technique avoids the convergence difficulties due to the particle creation on the solid boundaries (see [Coquerelle and Cottet 08] and [Cottet and Maitre 04]). Defining the Reynolds number as $\mathrm{Re} = u_{ref}\; l_{ref}/\nu$, the non-dimensional penalized vorticity equation reads

$$\frac{\partial\omega}{\partial t} + (\mathbf{u}.\nabla)\omega = (\omega\cdot\nabla)\mathbf{u} + \frac{1}{\mathrm{Re}}\Delta\omega + \lambda\nabla\times[\chi_S(\bar{\mathbf{u}} - \mathbf{u})], \tag{3}$$

where χ_S is the characteristic function that yields 0 in the fluid and 1 in the solid and $\bar{\mathbf{u}}$ indicates the velocity of the solid body.

To discretize the penalized vorticity equation (3) in a vortex method, the equation is split in three substeps. At each time step, one successively solves the following equations:

$$\frac{\partial\omega}{\partial t} = \lambda\nabla\times(\chi_S(\bar{\mathbf{u}} - \mathbf{u})) \tag{4}$$

$$\frac{\partial\omega}{\partial t} + (\mathbf{u}\cdot\nabla)\,\omega = (\omega\cdot\nabla)\mathbf{u} + \frac{1}{Re}\Delta\omega \tag{5}$$

To solve (4) we use a an implicit scheme ([Coquerelle and Cottet 08]) and we set

$$\widetilde{\omega}^{n+1} = \nabla\times\left[\frac{u^n + \lambda\Delta t\chi_S\bar{\mathbf{u}}^n}{1 + \lambda\Delta t\chi_S}\right]. \tag{6}$$

where Δt is the time step. The right hand side above is evaluated by centered finite differences.

At this stage, grid vorticity above a certain cut-off is used to create particle at grid point locations and equation (5) is solved by a classical vortex-in-cell method [Cottet and Koumoutsakos 00]. The velocity field is obtained by solving

$$\Delta\psi = -\omega \tag{7}$$

with boundary conditions on the stream function ψ where $\mathbf{u} = \nabla\times\psi$. Particles are pushed with a RK4 time-stepping. Particles are then remeshed on the original grid using the following third order interpolation kernel

$$\Lambda_3(x) = \begin{cases} 0 & \text{if } |x| > 2 \\ \frac{1}{2}(2-|x|)^2(1-|x|) & \text{if } 1 \le |x| \le 2 \\ 1 - \frac{5x^2}{2} + \frac{3|x|^3}{2} & \text{if } |x| \le 1 \end{cases} \tag{8}$$

Finally diffusion is solved through an implicit solver on the grid, with a classical 7-points second order scheme. Note that the same kernel is used to interpolate grid velocity values onto particles in the RK4 particle pusher. Grid values for vorticity, velocity and level set functions are now available for time t_{n+1} and a new cycle of iterations can start. Moreover, the no-slip boundary conditions are naturally satisfied penalizing the vorticity transport equations.
In all the examples below we will consider bluff-body flows in domains that can be put in a rectangular box.

3 VALIDATION FOR THE FLOW AROUND A CIRCULAR CYLINDER

The literature about the classical benchmark of the 2D circular cylinder is wide. A deepened survey of this subject with several physical remarks and references therein can be found in [Williamson 96].

Here, we present some results of the numerical simulations of an incompressible flow past a 2D circular cylinder performed by the level set vortex method for different laminar and transitional Reynolds numbers in the range of $13 \le Re \le 9500$.

The computational domain and the geometrical setup are shown in figure 1, where D is a rectangle delimited by its boundaries Γ^D. The non-dimensional diameter d of the circular cylinder and the free stream inlet velocity u_∞ are equal to 1. The Reynolds number is defined as $\mathrm{Re} = u_\infty d/\nu$. The whole computational domain is meshed by an equispaced Cartesian orthogonal grid.

For the subsequent simulations of the wake past the circular cylinder, the flow field is computed solving the Poisson equation 7 with a Neumann condition at downstream Γ^D_{DA} and upstream Γ^D_{BC} and a Dirichlet condition of the streamfunction over Γ^D_{AB} and

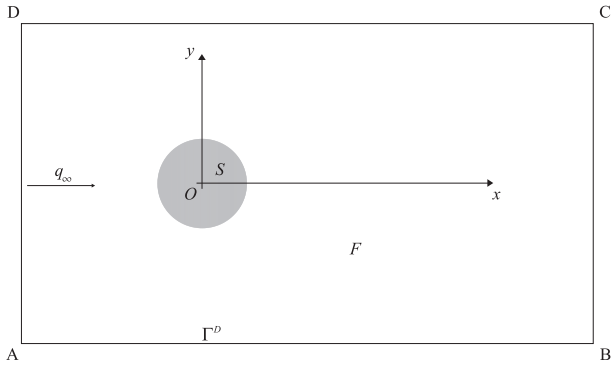

Figure 1: Computational domain $D = F \cup S$, where F is the fluid region and S is the solid body region.

Γ^D_{CD}. In particular, around the cylinder a potential flow condition is considered and the value of the associated streamfunction is enforced over Γ^D_{AB} and Γ^D_{CD}, that is

$$\psi = q_\infty y\left(1 - \frac{(d/2)^2}{x^2+y^2}\right). \tag{9}$$

The uniform flow q_∞ is used for initialization.

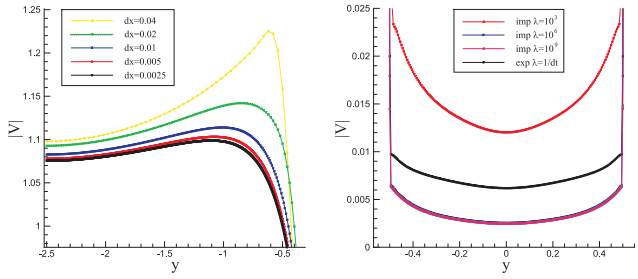

Figure 2: Convergence on grid test (left). Effect of the penalization parameter λ (right).

First of all, the grid convergence of the hybrid penalization-vortex code is verified, considering an impulsively started cylinder flow with $\mathrm{Re} = 550$. The figure 2 shows the l^2-norms of the instantaneous velocity values for different grid sizes and penalization parameters at time $t = 3$. The first plot is performed for a section at $x_s = 1.5$ with $\lambda = 10^{10}$ and the second one for a section at the middle of the cylinder ($x_s = 0.0$) with a mesh size $h = 0.005$. As the figure shows the velocity profiles converge towards a single curve increasing the grid refinement, Also, we see that increasing the penalization coefficient the profiles join the explicit result and confirm the previous analytical

observations. Practically, the explicit penalization needs to use $\lambda \leq 1/\Delta t$, whereas the implicit penalization is unconditionally stable.

Then, we focus on the low Reynolds number analysis where the viscous effects are predominant and without the onset of $3D$ instabilities the flow has a two-dimensional behavior. Following [Ploumhans and Winckelmans 00] the non-dimensional time-step Δt is determined by the condition $\Delta t/(h^2\ \mathrm{Re}) \sim O(1)$.

Various tests have been carried out by increasing the blockage ratio $d/(y_D - y_A)$, and a growth of the shedding frequency has been noticed. The size of the computational domain is chosen such that the effects of the boundaries on the shedding frequencies are negligible. The subsequent simulations have been performed on a flow region with dimensions $[-7.5,\ 25] \times [-7.5,\ 7.5]$ with 3250×1500 grid points ($h = 0.01$). The penalization is introduced using the implicit formulation 6 and the penalization parameter is $\lambda = 10^{10}$. Here, the flow regime is laminar, the solution is steady and stable for $\mathrm{Re} < \mathrm{Re}_{crit} = 49$ ([Williamson 96]). In figure 3, the streamlines for the steady solution at $Re = 13.05$ are shown. On the left-hand side, a picture of an experimental visualization is reported (see [Van Dyke 82]) and the equivalent frame computed by the present method is shown on the right-hand side. As the figure shows the steady recirculation areas have the same size and shape.

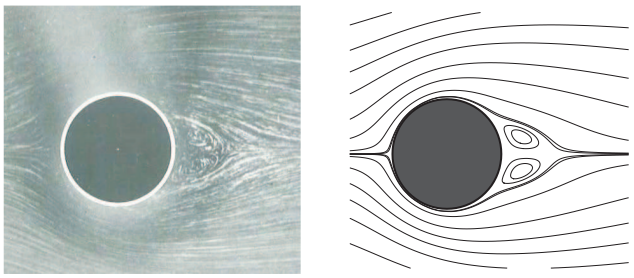

Figure 3: Streamlines at $Re = 13.05$

Increasing the Reynolds number, the flow regime is still laminar but the steady solution becomes unstable ($\mathrm{Re} > \mathrm{Re}_{crit}$). On the left-hand side picture of the figure 4, the amplitude A_ω of the fluctuation of the vorticity on a monitoring point $P = (2.5,\ 0.5)$ is plotted for varying Re. For a flow regime close to the bifurcation point Re_{crit} ($\mathrm{Re} < 60$) the wake instabilities grow very slowly, so the oscillation study is started at $Re = 60$. Nevertheless, the exact critical Reynolds number is obtained with a linear extrapolation of the amplification factor curve. Taking the Strouhal number $\mathrm{St} = fd/u_\infty$, where f is the vortex shedding frequency, the numerical and the experimental ([Williamson 96]) St *versus* *Re* curve is plotted on the right-hand side of the figure 4. An estimation of the average relative error ε between the curves yields $\varepsilon \approx 0.6\%$.

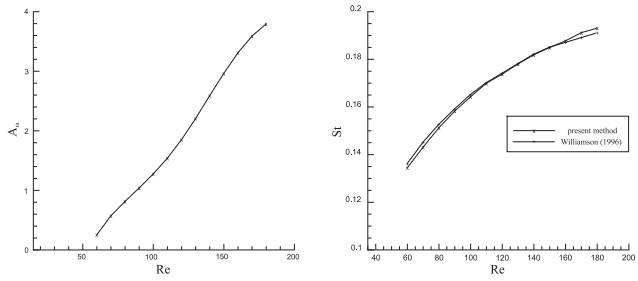

Figure 4: Amplification factor A_ω curve (left). Strouhal-Reynolds curve (right).

The evaluation of forces has been carried out using the 'momentum equation', as described in [Noca et al. 99]. Here, the mean values and the amplitudes of the fluctuations of drag and lift coefficients for flows at $\mathrm{Re} = 100$ ($\overline{C_D} = 1.40$, $\Delta C_D = 0.01$, $\Delta C_L = \pm 0.32$) and $\mathrm{Re} = 200$ ($\overline{C_D} = 1.44$, $\Delta C_D = 0.05$, $\Delta C_L = \pm 0.75$) are computed, where $\overline{C_D}$ is the mean drag coefficient and Δ corresponds to the amplitude of oscilations. These results are very close to experimental and numerical data collected by [Russel and Wang 03]. In figure 5, the time history of C_D and C_L for the flow past the circular cylinder at $\mathrm{Re} = 200$ is shown that are fitted to those obtained by Zdrakovich [Zdrakovich 97]. To take into account a transitional case we focus now on an impulsively started flow at $\mathrm{Re} = 550$ and compare the results to [Ploumhans and Winckelmans 00]. The time evolution of drag coefficients

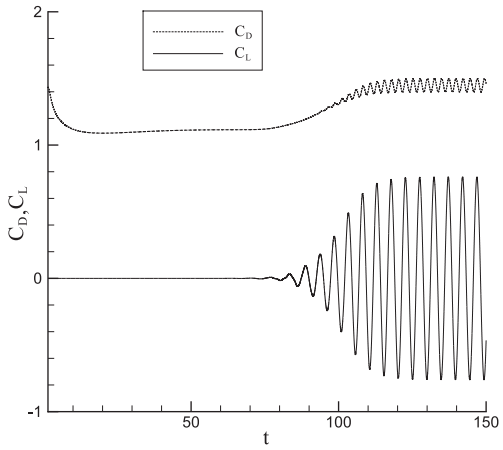

Figure 5: Time evolution of the drag and lift coefficients at $\mathrm{Re} = 200$.

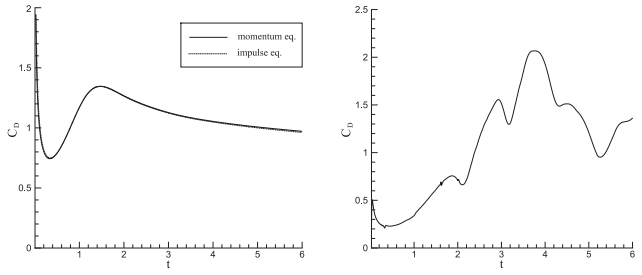

Figure 6: Time evolution of the drag coefficient for the impulsively started cylinder at Re = 550 (left) and at Re = 9500 (right).

are studied using the 'momentum equation' ([Noca et al. 99]) and the 'hydrodynamical impulse equation' ([Noca et al. 99]) methods, as shown on the left-hand side of the figure 6. It should be outlined that the 'hydrodynamical impulse' method needs a zero farfield velocity. Here, a Galilean transformation is used moving the body with a $-u_\infty$ velocity to achieve the correct boundary and force computations. Moreover, in order to avoid the reflecting effect of the outgoing vortices from the exit boundaries the computations are performed on a short time $t = 6$.

As the curve shows, the results have a very good coincidence. Also, they correspond to the drag computations obtained in [Ploumhans and Winckelmans 00]. The figure 7 shows the vorticity iso-contours which are very similar to the vorticity field presented by Ploumhans & Winckelmans, introducing accurately the separation contours and the recirculation area sizes. Here, the grid convergence in a computational domain $[-3.75,\ 12.5] \times [-3.75,\ 3.75]$ is achieved with parameters $h = 0.005$ and $\lambda = 10^9$.

The last simulation is carried out for the flow around the impulsively started cylinder at Re = 9500 and compared to numerical results obtained by [Koumoutsakos and Leonard 95]. For such a high Reynolds number, the flow is unstable and the shedding generates complex vortex pairings (see [Williamson 96]). Taking a domain $[-1.5,\ 4.5] \times [-2.5,\ 2.5]$, the grid convergence is achieved for $h = 0.0025$ and $\lambda = 10^9$. Since at large Reynolds numbers the flow is dominated by convection, the time-step is not chosen by the condition $\Delta t/(Re\ h^2) \sim O(1)$, but its value is reduced to $\Delta t = 0.005$ in order to achieve the numerical accuracy. According to [Williamson 96], the time is non-dimensionalized and is based on the cylinder radius. On the right-hand side of figure 6 the evolution in time of the drag coefficient, computed using the 'momentum equation', is reported. The result is very similar to the corresponding curve in [Koumoutsakos and Leonard 95] . Finally, on figure 8, six snapshots ($t = 1,\ 1.5,\ 2,\ 2.5,\ 3,\ 3.5$) of the of vorticty field are ploted and a good agreement with Koumoutsakos & Leonard (1995) is observed.

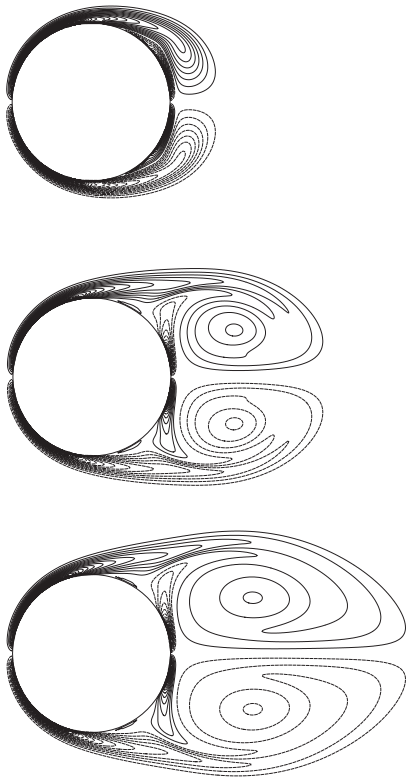

Figure 7: Iso-contours of vorticity for $t = 1,\ 3,\ 5$ for the impulsively started cylinder at Re = 550.

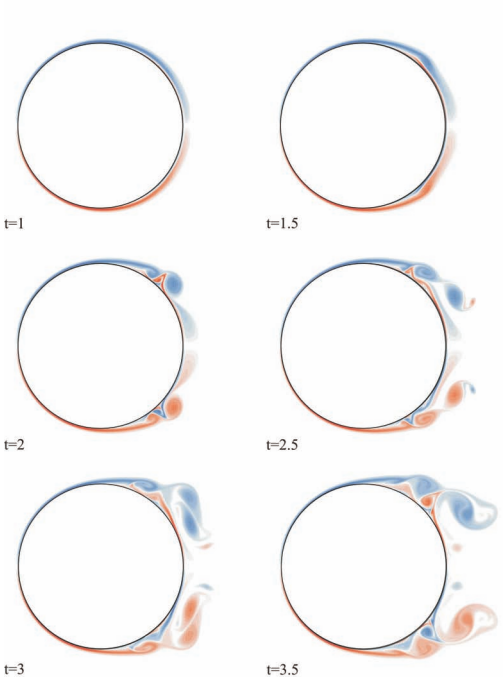

Figure 8: Iso-contours of vorticity for $t = 1,\ 1.5,\ 2,\ 2.5,\ 3,\ 3.5$ for the impulsively started cylinder at Re = 9500.

4 CONCLUSIONS

In the first part of this paper, A hybrid vortex-penalization method was described in order to achieve an accuarte and fast approximation of incompressible vortex flows around bluff-bodies. In this algorithm the penalization method replaces the classical sheet generation approach of vortex methods in order to satisfy the no-slip boundary conditions. The new method not only avoids a *heuristic* estimation of vorticity generation on solid boundaries but also corresponds to an immersed boundary technique generating simplified body fitting trends with moving obstacles. Then, the technique was validated to laminar, transitional and turbulent flows around a circular cylinder achieving a good agreement with former experimental and numerical studies.

REFERENCES

[Angot et al. 1999] Angot Ph., Bruneau Ch.-H., Fabrie P., *A penalization method to take into account obstacles in incompressible viscous flows*, Numer. Math. **81**, 1999.

[Bruneau et al. 2008] Bruneau Ch.-H., Mortazavi I., Gilliéron P., *Passive control around the two-dimensional square back Ahmed body using porous devices*, J. Fluids Eng. **130**, 2008.

[Cottet and Koumoutsakos 00] Cottet G. H., Koumoutsakos. P., *Vortex Methods: Theory and Practice*, Cambridge University Press, 2000.

[Cottet and Maitre 04] Cottet, G. -H. and Maitre, E., *A level-set formulation of immersed boundary methods for fluid-structure interaction problems*, C. R. Acad. Sci. Paris, **338**, 2004.

[Noca et al. 99] Noca, F. and Shiels, D. and Jeon, D., *A comparison of methods for evaluating time-dependent fluid dynamic forces on bodies, using only velocity fields and their derivatives*, Journal of Fluids and Structures **13**, 1999.

[Williamson 96] Williamson, C. H. K., *Vortex dynamics in the cylinder wake*, Annual Review of Fluid Mechanics **28**, 1996.

[Ploumhans and Winckelmans 00] Ploumhans, P. and Winckelmans, G. S., *Vortex methods for high-resolution simulations of viscous flow past bluff bodies of general geometry*, Journal of Computational Physics **165**, 2000.

[Koumoutsakos and Leonard 95] Koumoustakos, P. and Leonard, A., *High-resolution simulations of the flow around an impulsively started cylinder using vortex methods*, Journal of Fluid Mechanics **296**, 1995.

[Russel and Wang 03] Russell, D. and Wang, Z. J., *A cartesian grid method for modeling multiple moving objects in 2D incompressible viscous flow*, Journal of Computational Physics **191**, 2003.

[Coquerelle and Cottet 08] Coquerelle, M. and Cottet, G. -H., *A vortex level set method for the two-way coupling of an incompressible fluid with colliding rigid bodies*, Journal of Computational Physics **227**, 2008.

[Coquerelle et al 06] Coquerelle, M. and Allard, J. and Cottet, G. -H. and Cani, M. -P., *A Vortex Method for Bi-phasic Fluids Interacting with Rigid Bodies*, Arxiv preprint math, LMC-IMAG, 2006.

[Mortazavi and Giovannini 01] Mortazavi, I. and Giovannini, A., *The simulation of vortex dynamics downstream of a plate separator using a vortex-finite element method*, International Journal of Fluid Dynamics, **5**, 2001.

[Van Dyke 82] van Dyke, M., *An album of fluid motion*, Stanford: The Parabolic Press, 1982.

[Zdrakovich 97] Zdrakovich, N. M., *Flow around circular cylinders (Vol 1: Fundamentals)*, Oxford Science Publications, 1997.